Age-Dependent Changes in Total and Free Water Content of In Vivo Human Lenses Measured by Magnetic Resonance Imaging

Alyssa L. Lie,[1] Xingzheng Pan,[1,2] Thomas W. White,[3] Ehsan Vaghefi,[1] and Paul J. Donaldson[2]

[1]School of Optometry and Vision Science, New Zealand National Eye Centre, University of Auckland, New Zealand
[2]Department of Physiology, School of Medical Sciences, New Zealand National Eye Centre, University of Auckland, New Zealand
[3]Department of Physiology and Biophysics, Stony Brook University, Stony Brook, New York, United States

Correspondence: Paul J. Donaldson, Department of Physiology, School of Medical Sciences, New Zealand National Eye Centre, University of Auckland, New Zealand; p.donaldson@auckland.ac.nz.

Received: February 17, 2021
Accepted: April 14, 2021
Published: July 22, 2021

Citation: Lie AL, Pan X, White TW, Vaghefi E, Donaldson PJ. Age-dependent changes in total and free water content of in vivo human lenses measured by magnetic resonance imaging. *Invest Ophthalmol Vis Sci.* 2021;62(9):33. https://doi.org/10.1167/iovs.62.9.33

Purpose. To use magnetic resonance imaging (MRI) to measure age-dependent changes in total and free water in human lenses in vivo.

Methods. Sixty-four healthy adults aged 18 to 86 years were recruited, fitted with a 32-channel head receiver coil, and placed in a 3 Tesla clinical MR scanner. Scans of the crystalline lens were obtained using a volumetric interpolated breath-hold examination sequence with dual flip angles, which were corrected for field inhomogeneity post-acquisition using a B1-map obtained using a turbo-FLASH sequence. The spatial distribution and content of corrected total (ρ_{lens}) and free (T1) water along the lens optical axis were extracted using custom-written code.

Results. Lens total water distribution and content did not change with age (all $P > 0.05$). In contrast to total water, a gradient in free water content that was highest in the periphery relative to the center was present in lenses across all ages. However, this initially parabolic free water gradient gradually developed an enhanced central plateau, as indicated by increasing profile shape parameter values (anterior: 0.067/y, $P = 0.004$; posterior: 0.050/y, $P = 0.020$) and central free water content (1.932 ms/y, $P = 0.022$) with age.

Conclusions. MRI can obtain repeatable total and free water measurements of in vivo human lenses. The observation that the lens steady-state free, but not total, water gradient is abolished with age raises the possibility that alterations in protein-water interactions are an underlying cause of the degradation in lens optics and overall vision observed with aging.

Keywords: magnetic resonance imaging, crystalline lens, T1 mapping, water content, in vivo, aging

Throughout adulthood, the human eye undergoes multiple changes in overall visual function, the majority of which are associated with changes to the refractive and transparent properties of the crystalline lens.[1] Perhaps the most striking of these age-related changes are presbyopia in middle age[2,3] and cataract in the elderly,[4] which are manifestations of a loss of lens elasticity and transparency, respectively. A more subtle phenomenon that occurs to overall vision is the gradual shift in refractive status of the adult eye toward hyperopia,[5–11] which has been attributed to a decline in the refractive power of the lens with age, known as the "lens paradox" because of the counterintuitive nature in which the lens loses power.[12,13] Continual lifelong growth of the lens leads to a thicker and rounder shape with age,[14–16] so if one assumes the internal refractive index gradient (GRIN) remains constant, these geometric changes should over time result in a more powerful lens. The fact that the opposite occurs[3,17–19] suggests that aging processes alters the lens GRIN to counter the effects of lens growth on its geometry to produce a less-powerful lens.

Extensive work has demonstrated the lens GRIN does indeed change with age,[18–25] but there remains considerable debate regarding the underlying physiological mechanisms responsible for this change. Most recently, we used magnetic resonance imaging (MRI) to noninvasively obtain the GRINs of a wide age range of human lenses in vivo[26] and incorporated these values into an optical modeling platform that attempted to predict the clinically-measured visual performance of each subject. Our findings showed that the incorporation of an age-dependent factor into the MRI transverse relaxation time T2 versus refractive index (T2-*n*) calibration[18] was necessary to accurately model the measured refractive error. The need for the age-dependent factor indicates that with advancing age the contribution of lens proteins to the refractive index changes. Because T2 measures the water-to-protein ratio, this implies that aging

Investigative Ophthalmology & Visual Science

alters the way water interacts with proteins in the different regions of the lens.

Within the lens, water can be classed as being either protein-bound or free. The interactions between water and protein define which conformational state proteins will adopt[27] and are thus considered integral for proteins to maintain their refractive index increment. Given the importance of water in protein structure and function, an imbalance in the steady-state bound and free water proportions within the lens would be expected to produce downstream effects on the refractive properties of the lens. Indeed, a progressive increase in the ratio of free-to-bound water has been observed to occur with age,[28–30] and this has been correlated to a concurrent decrease in the refractive index of the lens, especially in the nucleus.[19,20,24] Alterations in lens hydration state have also been implicated in the loss of transparency of the lens. Cataractous lenses have been found to contain higher amounts of free water compared to clear lenses,[30,31] and an increased movement of water from a bound to a free state in opaque compared to transparent regions of the same lens has also been reported.[32,33] Furthermore, the lens has been shown to, at steady-state, actively maintain a gradient of free water concentration such that it is highest in the cortex relative to the nucleus.[34–36] Our laboratory has previously demonstrated through a series of studies on organ-cultured bovine lenses that pharmacologically dissipating the inherent free water gradient had the effect of altering the lens optical properties,[37] raising the question whether a similar redistribution of the steady-state free and bound water gradients occurs with aging in the human lens. Finally, there has also been speculation about an overall dehydration (i.e., loss of total water consisting of both free and bound components) of the lens with age; however, the existing literature is incomplete and contradictory. Although most studies report a relative dehydration of the lens with age,[30,31,38,39] others have reported that lens total water content does not change[29,40,41] or even increases with age.[42] It should also be noted that majority of the investigations into the various aspects of lens hydration to date have been performed on isolated ex vivo human lenses using destructive methods.

Therefore the purpose of this study was to develop noninvasive MRI protocols that would allow us to determine how free and total water changes with age in the in vivo human lens. MRI parametric mapping based on proton density (PD) and longitudinal relaxation time (T1) measurements have been extensively used to measure water in brain imaging[43] for detecting neurological diseases such as stroke[44] and multiple sclerosis.[45–47] Because PD measurements relate to the total number of hydrogen protons, which are predominantly resident in water molecules, it is often seen as a short-hand way of quantifying the total water content of the imaged tissue.[43] Because of their ultrashort transverse relaxation times (on the order of microseconds), protons that reside on macromolecules undergo a rapid signal decay and therefore cannot be probed using conventional MRI.[48] Because only protons that are bound to proteins or in the free water pool are included, PD measurements can be used to infer lens total water content. On the other hand, the T1 time constant is related to the dispersion of the excess energy of protons to the surrounding environment. Hence, T1 values provide information about the mobility of water molecules within the imaged tissue and can be used for quantifying free water within the lens. Using an optimized MRI protocol on the basis of these techniques, we show that, while increasing age had no discernible effects on the distribution or amount of total water in the lens, a plateau developed in the central region of the free water gradient and there was an increase in the free water content of the nucleus. These observations show that with advancing age the ability of lens proteins to bind water changes and suggests that changes in free water could be used as a biomarker of changes to the physiological optics of the lens.

Methods

Subjects

Sixty-four healthy adults (30 male, 34 female) aged between 18 to 86 years who had no visually-significant ocular pathologies (except mild cataract), prior intraocular surgery, diabetes mellitus, or contraindications for undergoing MRI were recruited for this study. All subjects had a mean sphere refractive error within ±6 diopters (D), and best-corrected visual acuities of at least 0.30 logMAR (Snellen 6/12). All procedures were approved by the University of Auckland Human Subjects Ethics Committee (reference: 017162) and complied with the tenets of the Declaration of Helsinki.

MRI Procedure and Post-Processing

All subjects were fitted with a 32-channel head receiver coil (Siemens, Munich, Germany) before undergoing MRI using a 3T clinical scanner (MAGNETOM Skyra; Siemens) located in the Centre for Advanced MRI at the University of Auckland. Inside the scanner, subjects laid supine on a table with their heads stabilized by foam pads. A falcon tube filled with room temperature water that served as an external water reference to obtain the relative fraction of the lens total water content[49] was strapped next to each subjects' eye (Fig. 1A). During the scan, subjects used a 45° tilted mirror attached to the head coil to view a fixation crosshair combined with pictures that randomly changed every five seconds,[26,50,51] giving a viewing distance of about 2.1 m.

In this study, PD- and T1-mapping of the lens were performed using a volumetric interpolated breath-hold examination sequence with dual flip angles (field of view = 159 mm; matrix size = 768 × 768; slice thickness = 3 mm; echo time [*TE*] = 2.7 ms; repetition time [*TR*] = 15 ms; flip angle [α] = 4° and 23°; parallel imaging acceleration factor = 2; total imaging time = 4.5 minutes). Post hoc field inhomogeneity correction of the raw MR images acquired at the two flip angles was then performed using a B1-map obtained by a turbo-FLASH sequence with pre-saturated preparation (field of view = 220 mm; matrix size = 160 × 160; slice thickness = 3 mm; *TE* = 2.23 ms, *TR* = 1349 ms; parallel imaging acceleration factor = 2; total imaging time = 30 s). The B1-map was resliced and coregistered with one volumetric set of images (α = 23°) for pixel-wise signal corrections.[52] Corrected PD and T1 maps were then calculated using the following MRI signal equation[53,54] (Equation 1):

$$\frac{S}{sin\,(\alpha b_1)} = \frac{S}{cos\,(\alpha b_1)} e^{-\frac{T_R}{T_1}} + PD\left(1 - e^{-\frac{T_R}{T_1}}\right) \qquad (1)$$

where S is the signal intensity, a is the flip angle, PD is the resting spin density before excitation (i.e., at time zero), and b_1 is a multiplier that denotes the ratio of actual flip angle (biased by field inhomogeneity) and ideal flip angle that is calculated from the acquired B1-map.[55]

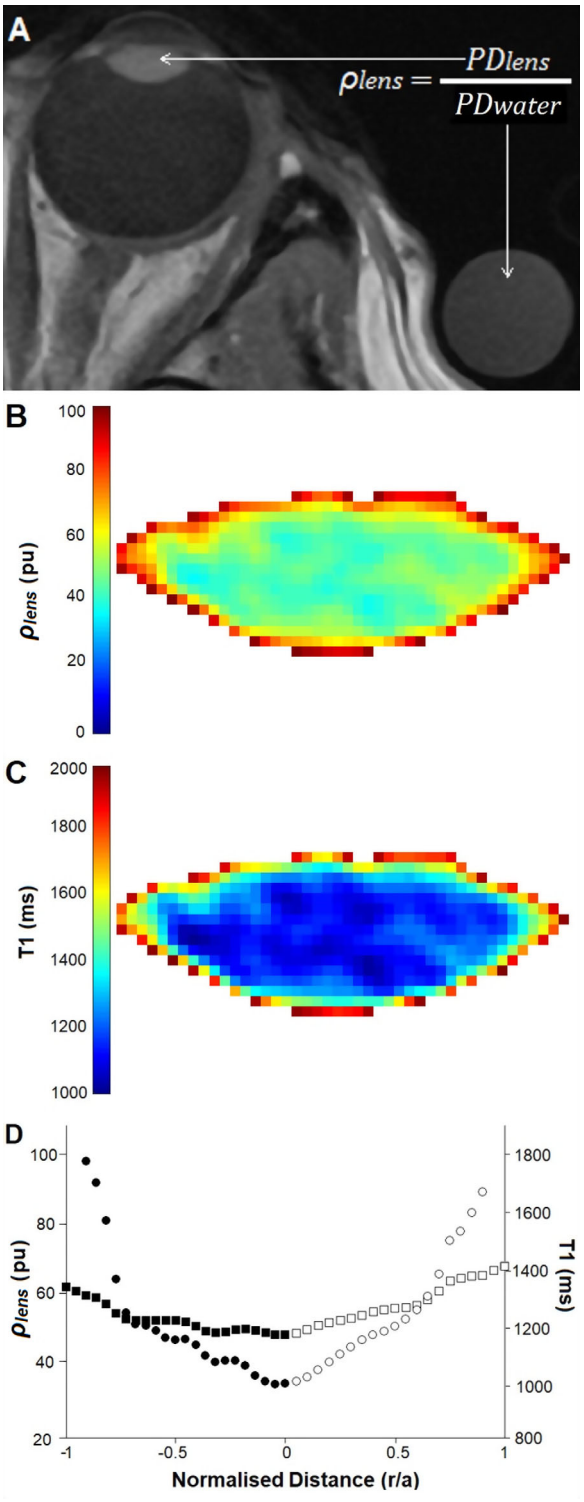

Figure 1. Postprocessing of human lens total water (ρ_{lens}) and free water (T1) distributions in vivo. (**A**) A raw MR image obtained of the left eye of a representative young subject, which includes a falcon tube of room temperature water that serves as an external water reference. This allows for the lens total water content (ρ_{lens}) to be calculated by normalizing the PD value of the lens (PD_{lens}) to that of the water tube (PD_{water}) using Equation 2. The lens was cropped from the eye and postprocessed using custom-written codes to generate 2-D PD (**B**) and T1 (**C**) color maps. (**D**) ρ_{lens} and T1 values were extracted along the optical axis and plotted against normalized distance (r/a) to give total water (*square*) and free water (*circle*) profiles. Profiles were then partitioned into the anterior (*filled*) and posterior (*empty*) regions and were then independently fitted from the lens center with Equation 3.

Corrected PD and T1 values of the lens were derived from the coefficients of the linear fitting performed between $\frac{S}{sin(\alpha b_1)}$ and $\frac{S}{cos(\alpha b_1)}$ to obtain the slope (i.e. $e^{-\frac{T_R}{T_1}}$) and the y-intercept (i.e., $PD(1-e^{-\frac{T_R}{T_1}})$).[56] The PD value of the external water reference (PD_{water}), which is representative of 100% water, was similarly calculated with Equation 1. The total water content of the lens (ρ_{lens}) was expressed as the relative fraction of the external water reference by normalizing the PD value of the lens (PD_{lens}) to PD_{water} as in Equation 2:

$$\rho_{lens} = \frac{PD_{lens}}{PD_{water}} \tag{2}$$

where ρ_{lens} is the total water content of the lens, described as a percentage unit of the external water reference (pu). Using this approach, instrumental factors such as different MRI manufacturers, field strength and radiofrequency coils are eliminated, giving the nontrivial measurement of the lens total water content.

For all MR images, the slice that contained the thickest cross-section of the lens visible was chosen for data extraction. All data processing was carried out using custom-written routines in MATLAB (MathWorks, Natick, MA, USA). A one-dimensional trend analysis was performed for each lens PD- and T1-map. For this, ρ_{lens} and T1 values over a 5-pixel-wide band along the lens optical axis were extracted, averaged and then fitted to a power function (Equation 3) going anteriorly and posteriorly from the lens center to give two independent profiles for total and free water from each subject's lens:

$$\rho_{lens}/T_1\ (r) = a + b(r)^c \tag{3}$$

where r is the normalized radial distance (r/a) from the lens surface, a is the total water (ρ_{lens}) or free water (T1) value at the lens center, b is the variation in ρ_{lens} or T1 between the lens center and surface (such that it is positive when water content is higher at the surface), and exponent c characterizes the rate of change in the ρ_{lens} or T1 profile gradients (i.e., the slope). Because water distribution along the equatorial axis is of limited relevance to the optics of the lens, its analysis was not included in this part of the study. The data extraction and fitting process are demonstrated in Figure 1.

Statistical Analysis

Linear regression of lens water parameters using age in years as the independent variable was performed to determine whether there was an age dependence. Right eyes were used in analyses unless it did not satisfy the inclusion criteria (one subject). All results were reported as mean ± standard deviation unless stated otherwise. All statistical analyses were performed using IBM SPSS Statistics (v25.0, IBM Corp. Armonk, NY, USA) and MATLAB, with a significance level of 5% used for all tests.

Results

We first present results for total (ρ_{lens}) and free (T1) water content obtained by applying our optimized in vivo MRI protocols to a small cohort of younger subjects to confirm the repeatability of our measurements. We then apply our methods to larger and older subject cohorts to assess how

Investigative Ophthalmology & Visual Science

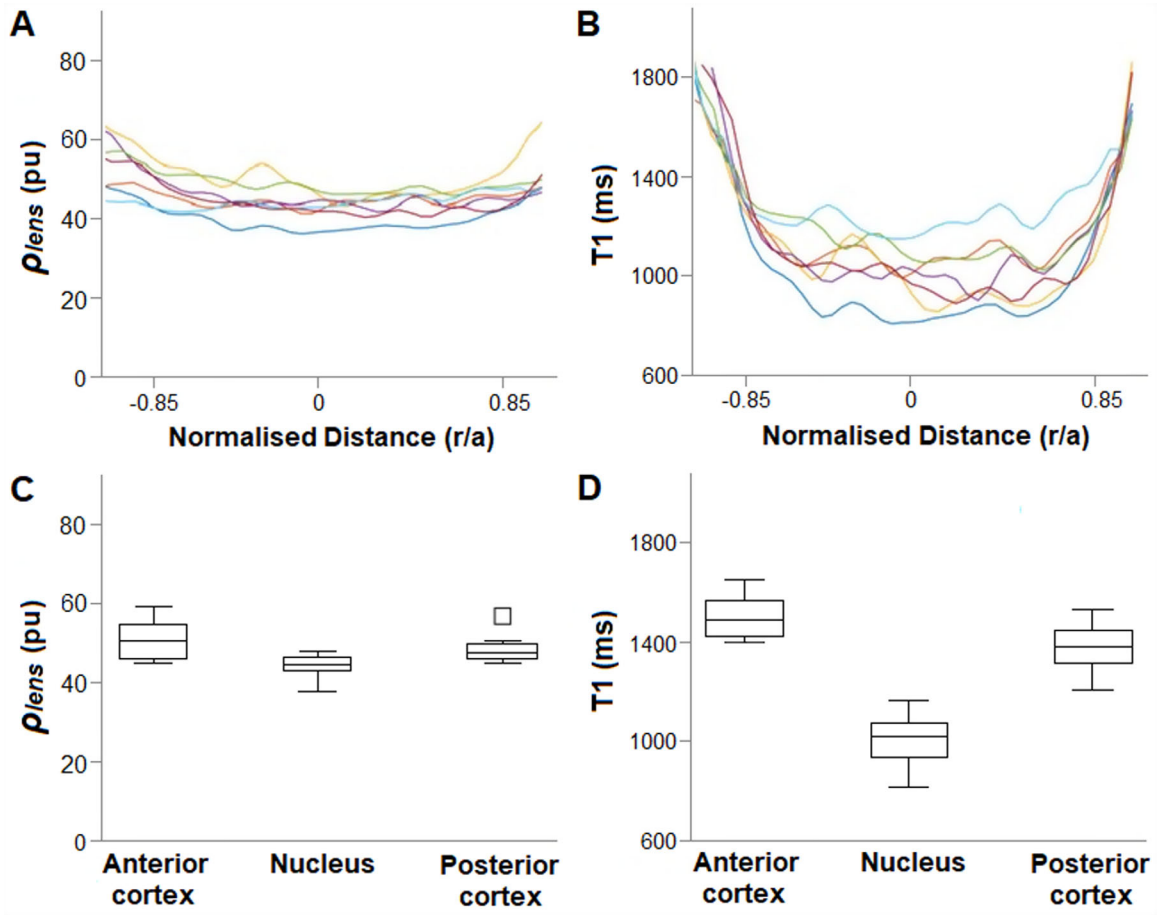

FIGURE 2. Analysis of total water (ρ_{lens}) and free water (T1) content in a subcohort of young lenses. Line profiles fitted to ρ_{lens} (**A**) and T1 (**B**) values extracted along the lens optical axis of seven young subjects. All ρ_{lens} profiles displayed a linear distribution where ρ_{lens} values were mostly similar across the whole lens axis, whereas T1 profiles displayed a parabolic distribution where T1 values from the lens periphery were higher than those in the lens center. Box plots showing the mean ρ_{lens} (**C**) and T1 (**D**) values obtained from regions of interest in the anterior cortex (r/a = −0.85), nucleus (r/a = 0) and posterior cortex (r/a = 0.85) of the lens. ρ_{lens} values showed lesser intersubject variability and were similar among the three regions. In contrast, despite intersubject variability in T1 values, cortical T1 values were still, on average, higher than nuclear T1 values.

the steady-state total and free water gradients change with advancing age in the human lens.

Validation of In Vivo Lens Water Measurements

To establish our protocols and test their repeatability, we first recruited a smaller cohort of seven young subjects (two males, five females; mean age: 28 ± 6 years). In this cohort, ρ_{lens} and T1 values were extracted as either total (Fig. 2A) or free (Fig. 2B) water profiles, respectively, across the optical axis or as mean values of total (Fig. 2C) and free (Fig. 2D) water obtained from three regions of interest defined as the anterior cortex (r/a = −0.85), the nucleus (r/a = 0), and the posterior cortex (r/a = 0.85). The total water profiles obtained for these young lenses were mostly linear (Fig. 2A), indicating that total water distribution across the lens is relatively constant. However, a repeated measures one-way analysis of variance revealed a slight but significant decrease (P = 0.016) in the mean total water content of the nucleus (43 ± 4 pu) relative to the anterior and the posterior cortex (both 47 ± 5 pu) (Fig. 2C). In contrast, the free water distribution across the optical axis varied considerably, exhibiting a parabolic shape (Fig. 2B). Free water content in the nucleus (970 ± 82 ms) was significantly lower relative to both the anterior (1459 ± 69 ms; $P < 0.005$) and posterior (1359 ± 102 ms; $P < 0.005$) cortex (Fig. 2D), with no significant difference being observed between the mean free water content of the two cortical regions (P = 0.163). Interestingly, although the variability of total water content between subjects was relatively small, presumably in part because of the normalization to an external water standard, considerably greater intersubject variability was observed for the T1 values that represent free water (Figs. 2B, 2D).

To rule out whether this observed intersubject variability in T1 values was due to MRI measurement error, the seven young subjects were rescanned at the same time of day (± 1 hour) up to five days after their initial scan. To evaluate test-retest repeatability of the lens free water measurements, both the shape of the T1 profiles (Fig. 3A) and the mean T1 values obtained in the different regions of the lens (Fig. 3B) were compared between scans using Pearson's correlation analysis, paired t-tests, and Bland-Altman plots. Within-subject coefficients of variation (CoV) were also calculated based on a within-subject standard deviation method.[57] These analyses showed that the shape parameter (exponent c) of the anterior and posterior free water profiles

Investigative Ophthalmology & Visual Science

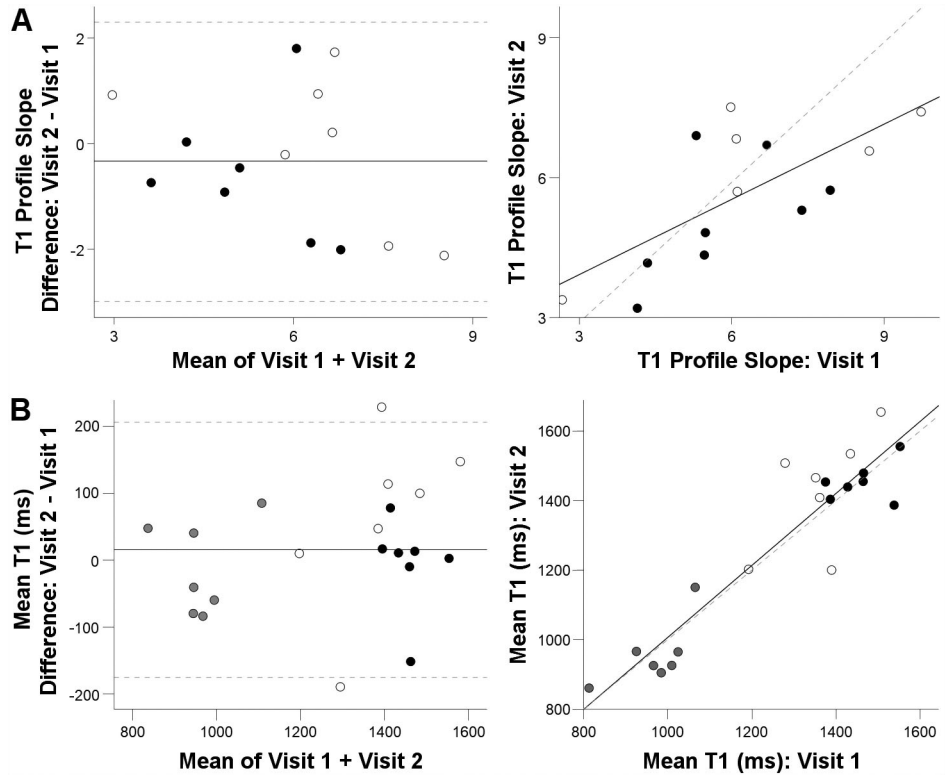

Figure 3. Validation of lens free water (T1) measurements in vivo in a cohort of young subjects. After an initial scan (Visit 1), the seven young subjects were rescanned (Visit 2) at the same time of the day (±1 hour), but up to five days after the first scan. (**A**) Correlation (*left*) and Bland Altman (*right*) plots of T1 profile slopes (shape parameter exponent *c*) fitted anteriorly (*filled circles*) and posteriorly (*empty circles*) from the lens center using Equation 3. (**B**) Correlation (*left*) and Bland Altman (*right*) plots of lens free water content (T1 values) at the anterior cortex (r/a = −0.85; *filled squares*), nucleus (r/a = 0; *shaded squares*), and posterior cortex (r/a = 0.85; *empty squares*). On the correlation plots, the *black solid line* indicates the best fit line, and the *dashed gray line* indicates the unity line. On the Bland-Altman plots, the *black solid line* indicates the mean bias, whereas the *dashed gray lines* indicate the upper and lower 95% limits of agreement.

obtained along the optical axis did not significantly differ (mean difference: −0.43 ± 1.36, 95% confidence interval [CI] [−1.22, 0.35], $P = 0.255$) between scans (Fig. 3A, *left panel*), whereas the correlation plot showed a strong agreement ($r = 0.693$, $P = 0.006$) between T1 profiles shapes between the two visits (Fig. 3A, *right panel*). The within-subject CoV was 16%. The free water content of the nucleus, anterior and posterior cortices also did not significantly differ (mean difference: 16 ± 97 ms, 95% CI [−29, 60] ms, $P = 0.470$) between the two MRI scan sessions (Fig. 3B, *left panel*). There was also a strong correlation between the regional free water content obtained at the two visits ($r = 0.927$, $P < 0.0005$), and the within-subject CoV was 5% (Fig. 3B, *right panel*). This confirms the repeatability of MRI protocols to measure lens water content and tends to suggest that the variability we have observed in lens free water is likely to be due to inherent intersubject biological variability.

Age-Dependent Changes in Lens Total and Free Water Content and Distribution

Having established and tested the repeatability of our MRI protocols to measure the lens water content and distribution in vivo on a subcohort of young subjects we then applied these protocols to a larger cohort of subjects, who had been previously recruited for another study,[26] to investigate how total and free water changes in the lens with age. Unfortunately, due to imaging artefacts, PD and T1 lens maps could not be extracted in four subjects (3 middle-aged and 1 older) and these subjects were excluded from further analysis. Hence, the effects of age on total and free water for 53 subjects are reported (Table).

Table. Descriptive Characteristics of the Final Subject Cohort (n = 53) Included in Analyses of Free and Total Water Changes in the Lens With Age

Characteristic	Young (18–40)	Middle-Aged (41–60)	Older (>60)
No.	22	17	14
Age (y)	24 ± 4	50 ± 5	73 ± 6
Male	10 (45%)	10 (59%)	5 (36%)
Refraction (D)	−1.52 ± 1.70	−0.77 ± 1.75	0.94 ± 1.55

Data are reported as either mean ± standard deviation (SD) or No. (%).

Total Water. Consistent with the PD profiles of lenses extracted from the smaller cohort of younger subjects, total water content (ρ_{lens}) remained relatively constant across the optical axis of young (Fig. 4A), middle-aged (Fig. 4B), and older (Fig. 4C) lenses, and the profiles did not appear to be influenced by aging (Fig. 4D). This was confirmed by plotting mean total water content obtained from the three regions of interest of the lens against subject age (Fig. 5). Total water content in the nucleus (Fig. 5A; $P = 0.617$),

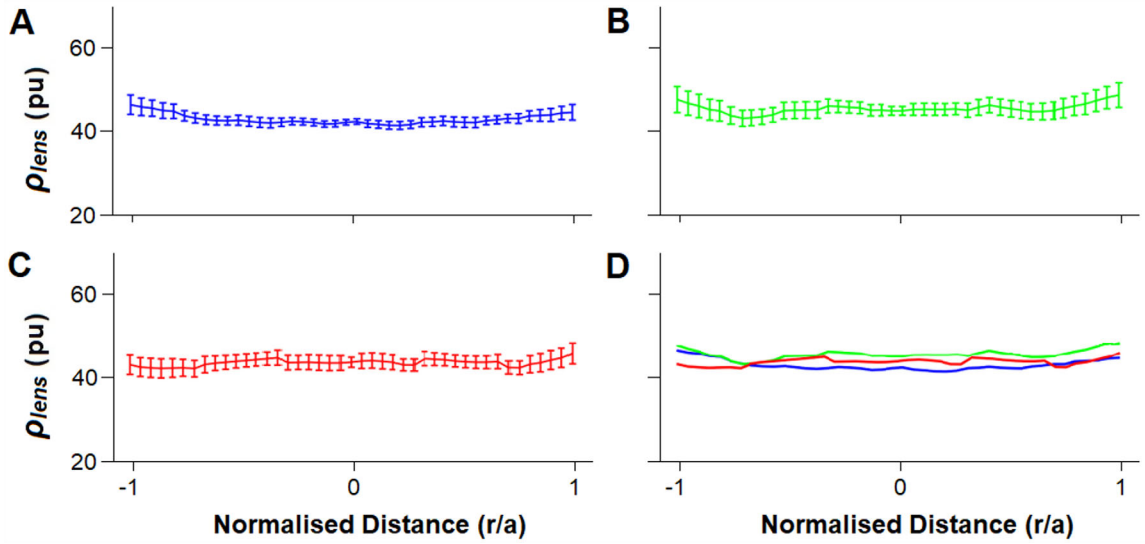

Figure 4. Differences in the distribution of total water (ρ_{lens}) in the human lens between age groups. Average profile plots of total water content (ρ_{lens} values) against normalized distance (r/a) extracted along the optical axis from lenses in young (**A,** *blue*), middle-aged (**B,** *green*), and older (**C,** *red*) age groups. *Error bars*: ±2 standard error. (**D**) Comparison of the average total water profiles obtained for each age group to emphasize that total water distribution does not markedly change with age.

anterior (Fig. 5B; $P = 0.482$) and posterior (Fig. 5C; $P = 0.781$) cortex showed no significant age dependency.

Free Water. Again, consistent with the T1 profiles of lenses extracted from the smaller cohort of younger subjects, free water content varied across the optical axis of young (Fig. 6A), middle-aged (Fig. 6B), and older (Fig. 6C) lenses, being highest in the periphery and lowest in the nucleus. Regardless of age, all subjects displayed a smooth gradient of free water that was lowest in the central region and increases toward the periphery. However, with advancing age the T1 profile across the lens optical axis developed a flattened central plateau, and the magnitude of T1 values measured in the central region was elevated (Fig. 6D). There was a significant increase (1.932 ms/y, $P = 0.022$) in central free water content with age (Fig. 7A). There was also a significant increase in the value of profile slope parameter exponent c in both the anterior ($P = 0.004$) and posterior ($P = 0.020$) lens T1 profiles at a rate of 0.067/y and 0.050/y, accordingly, indicating a sharper rate of incline in the free water gradient from the lens center to periphery with age (Fig. 7B).

Discussion

In this study we have optimized dual MRI parametric PD- and T1-mapping protocols to obtain for the first time total and free water gradients simultaneously in human lenses in vivo. Our technique demonstrated excellent interday repeatability of lens free water (T1) measurements (Fig. 3) and suggested that the observed variability in T1 values was due to inherent biological variability in free water content between subjects. Overall these result show that MRI can be used as a reliable tool for quantifying water distribution and content in the in vivo human lens.

Although our total and free water profiles yielded the expected distributions,[34–36,42,58] the paucity of comparable data obtained by independent methods makes it difficult to validate our in vivo measurements of water content. As mentioned earlier, most previous published work was obtained from ex vivo lenses using destructive methods that were based on exploiting differences in physical properties between free and bound water. Lens total water content obtained with these methods was reported to be approximately 65% to 70% of the tissue weight,[29,30,41] which is higher than that obtained in the present study (45-50 pu). A couple of factors potentially contribute toward this discrepancy in lens total water measurement. First, our PD measurements were referenced to an external standard representative of 100% water rather than tissue weight; so they will inherently differ because water has a different density from the lens tissue. Second, because of the temperature dependence of both the proton magnetization process[49] and the density of water, our reference standard at room temperature produces a higher MRI signal strength than if it were at body temperature like the lens. This results in an underestimation of our absolute PD values and explains why they are lower than the generally accepted values of lens total water content. Some authors have argued that PD measurements do not take into account tightly bound water,[59–61] and therefore total water content obtained by MRI is well below that obtained by invasive methods; however, these authors did not take into account the temperature dependence of the water MRI signal, which would account for much of the reported discrepancies.

Free water content in these studies was also typically represented as a percentage of lens total water, which is not directly comparable to the MRI longitudinal relaxation time T1 used in this study. Our average T1 values of the lens nucleus (996 ± 120 ms) and cortex (1107 ± 105 ms) are similar to those reported by studies employing nuclear magnetic resonance (NMR), a noninvasive technique that works on the same principles as MRI to measure free water content in tissues,[28,62–65] although NMR does not spatially resolve the regional variations in free water across the lens. The studies most comparable to our current work are those of Patz et al.[66] and Richdale et al.,[67] who have published nuclear T1 values of 1138 ms and 1270 ms, and cortical T1 values of 1413 ms and 1630 ms, respectively, obtained from MRI experiments. Although these studies broadly agree

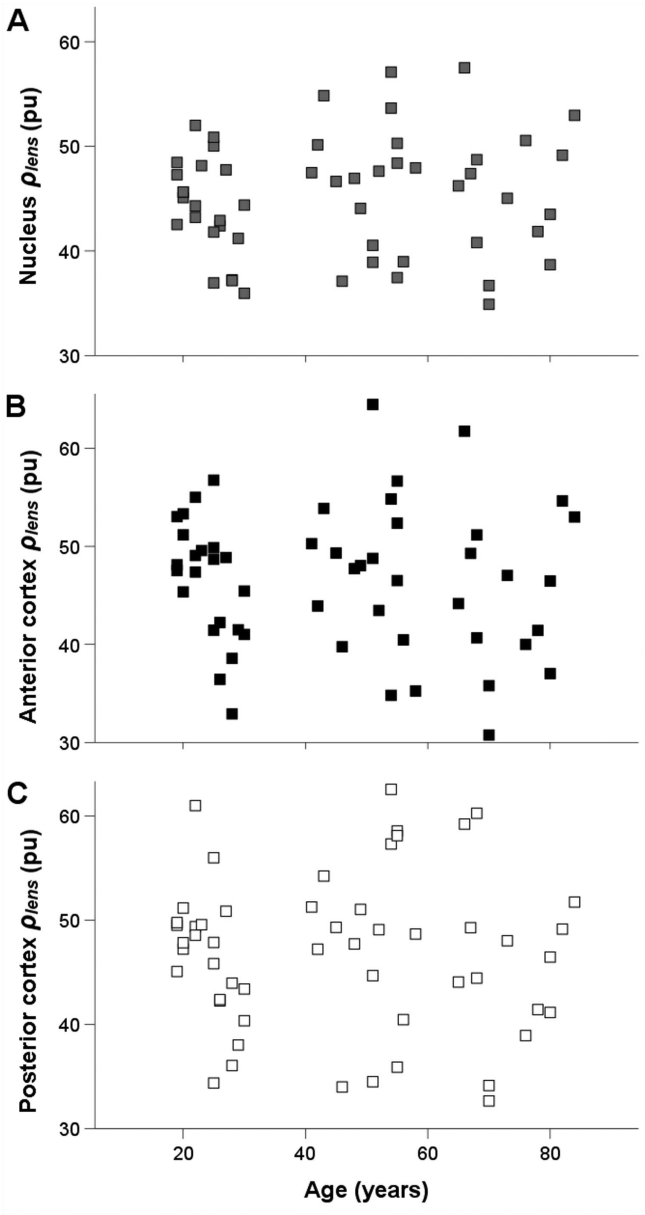

Figure 5. Effect of age on regional total water (ρ_{lens}) content in the human lens. Mean total water content (ρ_{lens} values) obtained from the lens (**A**) nucleus (r/a = 0; *shaded squares*), (**B**) anterior cortex (r/a = −0.85; *solid squares*), and (**C**) posterior cortex (r/a = 0.85; *empty squares*) plotted against age. No significant correlation between total water content and age was found in any of the three regions.

with our results, differences in imaging protocols (spin-echo sequence vs. variable flip angle), MRI field strengths (1.5T and 7T vs. 3T) and definitions of the nuclear and cortical regions (manual selection vs. predefined fractions) should be carefully considered given the dependence of T1 on these factors.[68]

Application of our optimized protocols to a larger and older subject cohort revealed that although increasing age had no discernible effects on total lens water content (Figs. 4, 5), an increase in the free water content of the lens nucleus and the development of central plateau in the free water profile occurred with increasing age (Figs. 6, 7). In a previous study performed on the same cohort of subjects,[26] similar age-related changes to the GRIN, but not T2, profile of the lens were found (Fig. 8). T2 values in the lens are dominated by proton exchange between bound water molecules and crystallin proteins; they can be used as a measure of the lens water-to-protein ratio (Fig. 8B) and for this reason should be correlated to the GRIN (Fig. 8C). However, our recent discovery that the same T2 values would yield different GRINs depending on age explains why the T2 profiles appear relatively unchanged in spite of an evident decrease in the lens central refractive index and development of a flattened central plateau in the GRIN profile between subject age groups. We previously hypothesized that this was most likely due to an age-dependent decrease in the refractive index increment of lens proteins, although it could also occur from an increase in lens total water or a loss in lens protein content. When taken together, our T1, T2, and GRIN measurements suggest that with age, the observed GRIN changes are driven by changes in the free water gradient, rather than changes in the lens total water or protein concentration. These observations therefore confirm that it is the interactions between protein and water that are altered with advancing age. Interestingly, these reciprocal age-dependent changes in the free water gradient and GRIN appear to contribute to the clinically observed lens paradox by reducing the optical power of the lens.[26]

Until now, it is not known whether the observed age changes in lens free and bound water proportions are a cause and/or effect of protein conformational changes in the lens. It has been postulated that the conversion of bound to free water does not occur solely as a simple consequence of the protein changes over that time period.[29] Although our observations do not inform us on how age alters the interaction between water and lens proteins that affects overall lens optics, we can speculate on two possible mechanisms. In the first, we envisage that the lifelong accumulation of posttranslational modifications to lens proteins[69–71] directly impairs their ability to bind water, causing an increase in free water content in the deeper areas of the lens where long-lived crystallin proteins are concentrated. In line with this, several protein modifications including truncation, oxidation, and deamidation have been identified in water-insoluble protein fractions of both clear and cataractous aged lenses.[72] The second possible mechanism involves age-related changes to the internal hydrostatic pressure gradient, which has been measured in all lenses studied to date.[73,74] This pressure gradient is generated by the outward movement of water through an intracellular pathway mediated by gap junction channels that is driven by the lens microcirculation system.[75–77] It has been revealed that this pressure gradient is regulated by a dual feedback system, which uses the mechanosensitive channels TRPV1 and TRPV4 to sense changes in pressure at the lens surface.[78] The realization that the lens pressure gradient is subject to feedback regulation[78] raises the possibility that age-related changes in this internal pressure gradient affect protein hydration in the lens nucleus.

Before the discovery of the internal hydrostatic pressure gradient, it was predicted on theoretical grounds that the lens undergoes reversible "syneresis" between the protein-bound state and surrounding free water as an operative response to changes in hydrostatic pressure.[79] A series of experiments by Bettelheim et al.[79–81] showed that applying external pressure to the lens surface causes a "reversed" syneresis, where free water enters the hydration shell around

Investigative Ophthalmology & Visual Science

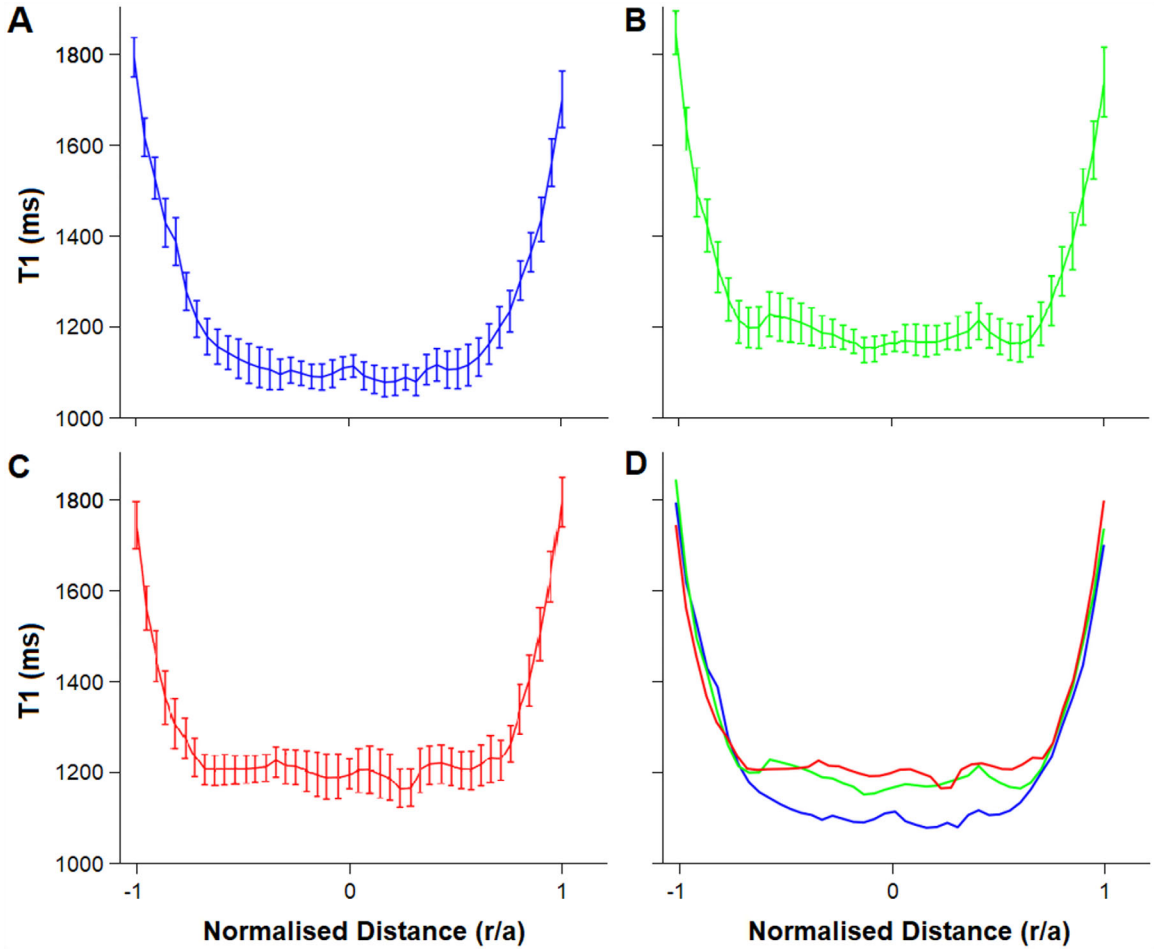

Figure 6. Differences in the distribution of free water (T1) in the human lens between age groups. Average profile plots of free water content (T1 values) against normalized distance (r/a) extracted along the optical axis from young (**A,** *blue*), middle-aged (**B,** *green*) and older (**C,** *red*) age groups. *Error bars*: ± 2 standard error. (**D**) Comparison of the average free water profiles obtained for each age group shows that free water content and distribution both change with age.

polar protein domains to become "bound," decreasing the lens free-to-bound water ratio. When the pressure was alleviated, this movement of water molecules is reversed and the free-to-bound water ratio increased. However, the extent to which water molecules in the lens undergo reversed syneresis in response to increasing pressure was found to diminish with age, and is actually reversed in older lenses (i.e., converts from bound to free). The relevance of this finding to aging was not fully recognized at the time, because it was thought that the pressure values tested were larger than those experienced by the lens in vivo.[82] Consistent with this notion, an age-dependent increase in endogenous hydrostatic pressure gradient has been reported in mice lenses,[73] but whether this also occurs in humans is yet to be determined. Of course, because protein hydration depends on protein structure (and vice versa), age-dependent modifications of lens proteins may also affect the ability of proteins to engage in syneresis. Hence, to fully understand the mechanisms responsible for the disruption of steady-state free water distribution and content and their implications on lens optics, the relative contributions of the lens physiology (pressure gradient) and protein structure to syneresis need to be further delineated.

Although free water in all lenses had the same parabolic distribution (Fig. 2B), large intersubject variability in absolute values were observed (Fig. 2D). Having shown the repeatability of our MRI measurements (Fig. 3), we concluded that this variability was due to inherent biological variability in free water content that in turn reflects individual differences in the protein content and composition of the lens nucleus. Because they are first established during embryonic development,[83] we propose that the observed subject-specific lens free water content reflect differences in lens water transport mechanisms designed to compensate for these potential differences to achieve a consistent and appropriate nuclear refractive index and lens GRIN overall, obtained by either the active removal of free water from the nucleus or via the imposition of a pressure gradient that modulates the amount of water bound to proteins via syneresis. Furthermore, the awareness that pharmacological modulation of ciliary muscle tone to alter the zonular tension applied to the mouse lens, also alters the magnitude of the lens hydrostatic pressure gradient,[84] suggests that the GRIN can be subjected to external regulation presumably to modify lens power and therefore overall visual performance. In the nonaccommodating mouse lens, we posit this mechanism is used to adjust the

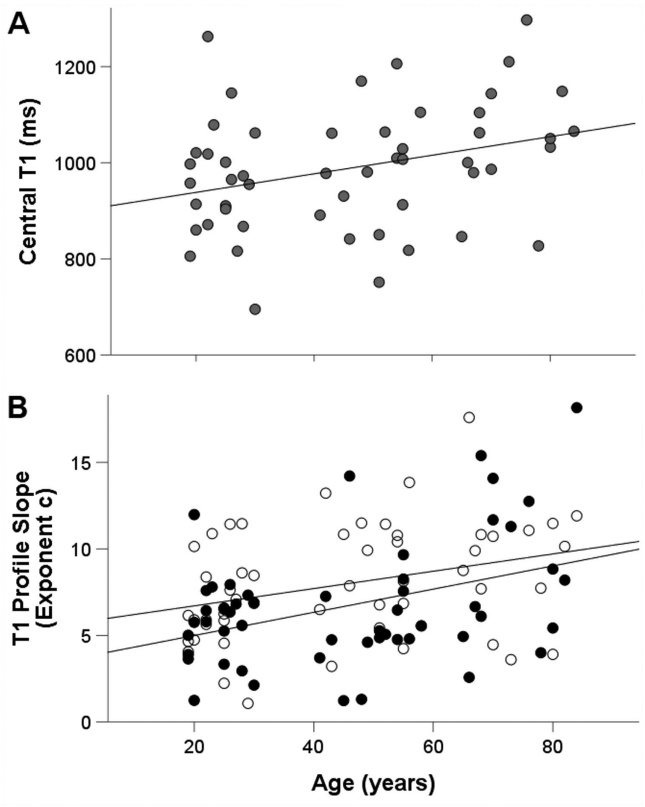

Figure 7. Effect of age on the content and distribution of free water (T1) in the human lens. (A) Mean free water content (T1 values) for obtained from lens nucleus (r/a = 0) plotted against age. There is a significant increase in central free water content with age: 899.576 + 1.932 × age (R^2 = 0.098, t = 2.355, n = 53, P = 0.022). (**B**) The slope of the free water profile (shape parameter exponent c) in the anterior (*solid circles*) and posterior lens (*empty circles*) plotted against age. There is a significant increase in the exponent value of both hemispheres, indicating a growing central plateau in the free water profile with age. Anterior: 3.652 + 0.067 × age (R^2 = 0.152, t = 3.024, n = 53, p = 0.004). Posterior: 5.705 + 0.050 × age (R^2 = 0.102, t = 2.410, n = 53, P = 0.020). All significant age trends are indicated by *solid lines*.

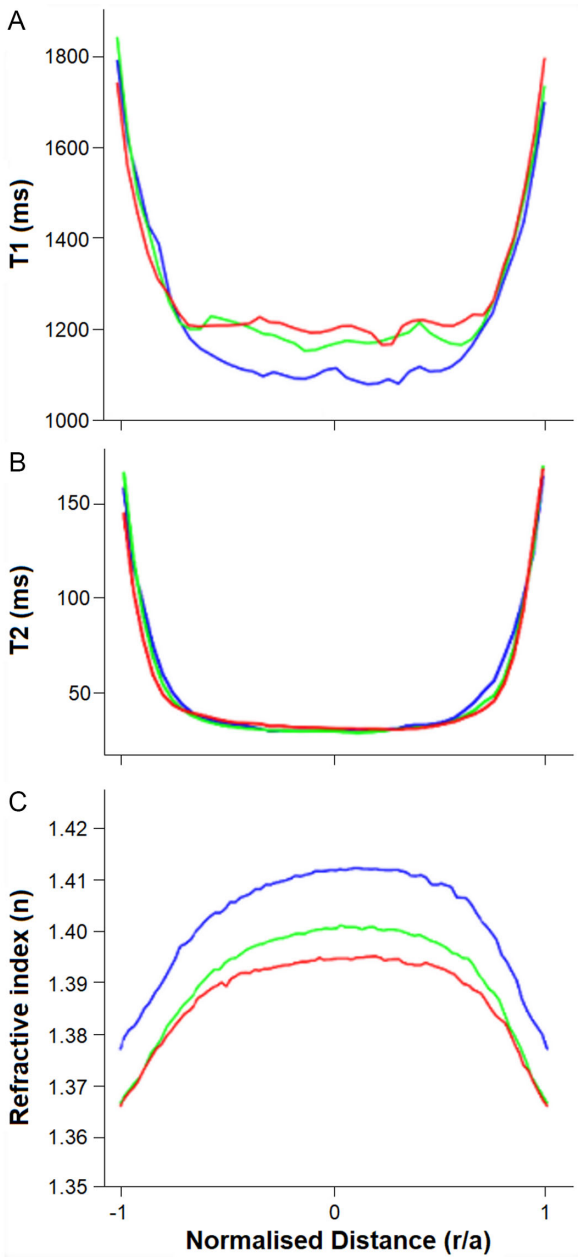

Figure 8. Summary of free water (T1), water-to-protein ratio (T2), and refractive index gradient (GRIN) profiles obtained from the same cohort of subjects. Comparison of the average profiles obtained for each age group shows distinct changes in free water (**A**) and GRIN (**C**), but not water-to-protein (**B**), distributions between young (*blue*), middle-aged (*green*), and older (*red*) subjects.

steady-state power of the lens as it grows throughout the lifetime of the animal. In humans, we anticipate a similar modulation of lens pressure would account for the age-dependent changes in its refractive power[3,17–19,26]; however, because the young human lens can accommodate, we also need to consider whether changes in zonular tension may be dynamically altering lens pressure and ergo, via syneresis, the free water distribution or content of the lens to drive the shape changes associated with accommodation.[85–87] It is possible that presbyopia occurs as a consequence of the diminished ability of the aging human lens to compensate for changes in zonular tension, and therefore hydrostatic pressure, during accommodation. This would not only explain the observed age-dependent increase in free water proportion within the lens, but also be expected to have implications on the stiffness and accommodative ability of the lens. The protocols developed in this study have the potential to test this hypothesis and will be the subject of future work.

In conclusion, by using optimized MRI protocols to spatially map the total and free water distribution and content of the lens, which act as in vivo physiological biomarkers of lens water transport, we have shown that changes to the free water population of the human lens are primarily responsible for the clinically observed changes in lens power and overall visual function that occur with age. Having established and tested the utility of MRI to study water content in the human lens in vivo, we expect that these protocols can be adapted to determine whether changes in lens water transport precede the onset of the age-related lens pathologies, presbyopia, and cataract.

Acknowledgments

The authors thank the volunteer subjects for their time. We also wish to thank the radiographers at CAMRI for their assistance

Investigative Ophthalmology & Visual Science

with performing MRI scans and Dr Safal Khanal for the opportunity to use his MRI fixation target.

Supported by funding from the National Institute of Health (NIH) Grant EY026911. During the period of this research study and preparation for publication, author ALL received doctoral scholarship support from the HOPE Selwyn Foundation and the New Zealand Association of Optometrists.

Disclosure: **A.L. Lie,** None; **X. Pan,** None; **T.W. White,** None; **E. Vaghefi,** None; **P.J. Donaldson,** None

References

1. Donaldson PJ, Grey AC, Maceo Heilman B, Lim JC, Vaghefi E. The physiological optics of the lens. *Prog Retin Eye Res*. 2017;56:e1–e24.
2. Glasser A, Campbell MCW. Presbyopia and the optical changes in the human crystalline lens with age. *Vis Res*. 1998;38:209–229.
3. Glasser A, Campbell MCW. Biometric, optical and physical changes in the isolated human crystalline lens with age in relation to presbyopia. *Vis Res*. 1999;39:1991–2015.
4. Asbell PA, Dualan I, Mindel J, Brocks D, Ahmad M, Epstein S. Age-related cataract. *Lancet*. 2005;365(9459):599–609.
5. Bomotti S, Lau B, Klein BEK, et al. Refraction and Change in Refraction Over a 20-Year Period in the Beaver Dam Eye Study. *Invest Ophthalmol Vis Sci*. 2018;59:4518–4524.
6. Lee KE, Klein BE, Klein R. Changes in Refractive Error over a 5-Year Interval in the Beaver Dam Eye Study. *Invest Ophthalmol Vis Sci*. 1999;40:1645–1649.
7. Lee KE, Klein BE, Klein R, Wong TY. Changes in refraction over 10 years in an adult population: the Beaver Dam Eye study. *Invest Ophthalmol Vis Sci*. 2002;43:2566–2571.
8. Fotedar R, Mitchell P, Burlutsky G, Wang JJ. Relationship of 10-year change in refraction to nuclear cataract and axial length findings from an older population. *Ophthalmology*. 2008;115:1273–1278.e1.
9. Guzowski M, Wang JJ, Rochtchina E, Rose KA, Mitchell P. Five-year refractive changes in an older population. *Ophthalmology*. 2003;110:1364–1370.
10. Goldblum D, Brugger A, Haselhoff A, Schmickler S. Longitudinal change of refraction over at least 5 years in 15,000 patients. *Graefes Arch Clin Exp Ophthalmol*. 2013;251:1431–1436.
11. Gudmundsdottir E, Arnarsson A, Jonasson F. Five-year refractive changes in an adult population: Reykjavik Eye Study. *Ophthalmology*. 2005;112:672–677.
12. Brown NP. The change in lens curvature with age. *Exp Eye Res*. 1974;19:175–183.
13. Brown NP, Koretz JF, Bron AJ. The development and maintenance of emmetropia. *Eye Lond*. 1999;13(Pt 1):83–92.
14. Atchison DA, Markwell EL, Kasthurirangan S, Pope JM, Smith G, Swann PG. Age-related changes in optical and biometric characteristics of emmetropic eyes. *J Vis*. 2008;8(4):291–320.
15. Dubbelman M, Van der Heijde GL. The shape of the aging human lens: curvature, equivalent refractive index and the lens paradox. *Vis Res*. 2001;41:1867–1877.
16. Koretz JF, Strenk SA, Strenk LM, Semmlow JL. Scheimpflug and high-resolution magnetic resonance imaging of the anterior segment: a comparative study. *J Opt Soc Am Opt Image Sci Vis*. 2004;21:346–354.
17. Borja D, Manns F, Ho A, et al. Optical power of the isolated human crystalline lens. *Invest Ophthalmol Vis Sci*. 2008;49:2541–2548.
18. Jones CE, Atchison DA, Meder R, Pope JM. Refractive index distribution and optical properties of the isolated human lens measured using magnetic resonance imaging (MRI). *Vis Res*. 2005;45:2352–2366.
19. Moffat BA, Atchison DA, Pope JM. Age-related changes in refractive index distribution and power of the human lens as measured by magnetic resonance micro-imaging in vitro. *Vis Res*. 2002;42:1683–1693.
20. Moffat BA, Atchison DA, Pope JM. Explanation of the lens paradox. *Optom Vis Sci*. 2002;79:148–150.
21. Jones CE, Atchison DA, Pope JM.Changes in lens dimensions and refractive index with age and accommodation. *Optom Vis Sci*. 2007;84:990–995.
22. Augusteyn RC, Jones CE, Pope JM. Age-related development of a refractive index plateau in the human lens: evidence for a distinct nucleus. *Clin Exp Optom*. 2008;91:296–301.
23. Kasthurirangan S, Markwell EL, Atchison DA, Pope JM. In vivo study of changes in refractive index distribution in the human crystalline lens with age and accommodation. *Invest Ophthalmol Vis Sci*. 2008;49:2531–2540.
24. Pierscionek BK, Bahrami M, Hoshino M, Uesugi K, Regini J, Yagi N. The eye lens: age-related trends and individual variations in refractive index and shape parameters. *Oncotarget*. 2015;6:30532–30544.
25. de Castro A, Siedlecki D, Borja D, et al. Age-dependent variation of the Gradient Index profile in human crystalline lenses. *J Mod Opt*. 2011;58:1781–1787.
26. Lie AL, Pan X, White TW, Donaldson PJ, Vaghefi E. Using the lens paradox to optimize an in vivo MRI-based optical model of the aging human crystalline lens. *Trans Vis Sci Tech*. 2020;9:39–39.
27. Bellissent-Funel M-C, Hassanali A, Havenith M, et al. Water determines the structure and dynamics of proteins. *Chem Rev*. 2016;116:7673–7697.
28. Bettelheim FA, Lizak MJ, Zigler JS, Jr. Relaxographic studies of aging normal human lenses. *Exp Eye Res*. 2002;75:695–702.
29. Heys KR, Friedrich MG, Truscott RJW. Free and bound water in normal and cataractous human lenses. *Invest Ophthalmol Vis Sci*. 2008;49:1991–1997.
30. Lahm D, Lee LK, Bettelheim FA. Age dependence of freezable and nonfreezable water content of normal human lenses. *Invest Ophthalmol Vis Sci*. 1985;26:1162–1165.
31. Bettelheim FA, Ali S, White O, Chylack LT. Freezable and non-freezable water content of cataractous human lenses. *Invest Ophthalmol Vis Sci*. 1986;27:122–125.
32. Bettelheim FA, Castoro JA, White O, Chylack LT. Topographic correspondence between total and non-freezable water content and the appearance of cataract in human lenses. *Curr Eye Res*. 1986;5:925–932.
33. Takemoto L, Sorensen CM. Protein-protein interactions and lens transparency. *Exp Eye Res*. 2008;87:496–501.
34. Moffat BA, Pope JM. Anisotropic water transport in the human eye lens studied by diffusion tensor NMR microimaging. *Exp Eye Res*. 2002;74:677–687.
35. Moffat BA, Landman KA, Truscott RJW, Sweeney MHJ, Pope JM. Age-related changes in the kinetics of water transport in normal human lenses. *Exp Eye Res*. 1999;69:663–669.
36. Vaghefi E, Pontre BP, Jacobs MD, Donaldson PJ. Visualizing ocular lens fluid dynamics using MRI: manipulation of steady state water content and water fluxes. *Am J Physiol Regul Integr Comp Physiol*. 2011;301:R335–R342.
37. Vaghefi E, Kim A, Donaldson PJ. Active maintenance of the gradient of refractive index is required to sustain the optical properties of the lens. *Invest Ophthalmol Vis Sci*. 2015;56:7195–7208.
38. Bours J, Födisch HJ, Hockwin O. Age-related changes in water and crystallin content of the fetal and adult human lens, demonstrated by a microsectioning technique. *Ophthalmic Res*. 1987;19:235–239.

Investigative Ophthalmology & Visual Science

39. Fisher RF, Pettet BE. Presbyopia and the water content of the human crystalline lens. *J Physiol*. 1973;234:443–447.
40. Heys KR, Cram SL, Truscott RJW. Massive increase in the stiffness of the human lens nucleus with age: the basis for presbyopia? *Mol Vis*. 2004;10:956–963.
41. Tabandeh H, Thompson GM, Heyworth P, Dorey S, Woods AJ, Lynch D. Water content, lens hardness and cataract appearance. *Eye Lond*. 1994;8(Pt 1):125–129.
42. Siebinga I, Vrensen GF, De Mul FF, Greve J. Age-related changes in local water and protein content of human eye lenses measured by Raman microspectroscopy. *Exp Eye Res*. 1991;53:233–239.
43. Tofts PS. PD: proton density of tissue water. In: Tofts P , editor. *Quantitative MRI of the Brain: Measuring Changes Caused by Disease*. Hoboken, NJ: John Wiley & Sons; 2003:85–108.
44. Gideon P, Rosenbaum S, Sperling B, Petersen P. MR-visible brain water content in human acute stroke. *Magn Reson Imaging*. 1999;17:301–304.
45. MacKay A, Whittall K, Adler J, Li D, Paty D, Graeb D. In vivo visualization of myelin water in brain by magnetic resonance. *Magn Reson Med*. 1994;31:673–677.
46. Whittall K, MacKay A, Graeb D, Nugent R, Li D, Paty D. In vivo measurement of T2 distributions and water contents in normal human brain. *Magn Reson Med*. 1997;37:34–43.
47. Vavasour IM, Whittall KP, Mackay AL, Li DKB, Vorobeychik G, Paty DW. A comparison between magnetization transfer ratios and myelin water percentages in normals and multiple sclerosis patients. *Magn Reson Med*. 1998;40:763–768.
48. Babizhayev MA, Nikolayev GN, Goryachev SN, Bours J. NMR spin-echo studies of hydration properties of the molecular chaperone alpha-crystallin in the bovine lens. *Biochim Biophys Acta*. 2002;1598(1-2):46–54.
49. Venkatesan R, Lin W, Gurleyik K, et al. Absolute measurements of water content using magnetic resonance imaging: Preliminary findings in an in vivo focal ischemic rat model. *Magn Reson Med*. 2000;43:146–150.
50. Pan X, Lie AL, White TW, Donaldson PJ, Vaghefi E. Development of an in vivo magnetic resonance imaging and computer modelling platform to investigate the physiological optics of the crystalline lens. *Biomed Opt Express*. 2019;10:4462–4478.
51. Thaler L, Schütz AC, Goodale MA, Gegenfurtner KR. What is the best fixation target? The effect of target shape on stability of fixational eye movements. *Vis Res*. 2013;76:31–42.
52. Preibisch C, Deichmann R. Influence of RF spoiling on the stability and accuracy of T1 mapping based on spoiled FLASH with varying flip angles. *Magn Reson Med*. 2009;61:125–135.
53. Blüml S, Schad LR, Stepanow B, Lorenz WJ. Spin-lattice relaxation time measurement by means of a TurboFLASH technique. *Magn Reson Med*. 1993;30:289–295.
54. Deoni SCL, Rutt BK, Peters TM. Rapid combined T1 and T2 mapping using gradient recalled acquisition in the steady state. *Magn Reson Med*. 2003;49:515–526.
55. Klose U. Mapping of the radio frequency magnetic field with a MR snapshot FLASH technique. *Med Phys*. 1992;19:1099.
56. Deoni SC, Peters TM, Rutt BK. Determination of optimal angles for variable nutation proton magnetic spin-lattice, T1, and spin-spin, T2, relaxation times measurement. *Magn Reson Med*. 2004;51:194–199.
57. Synek V. Evaluation of the standard deviation from duplicate results. *Accreditation Qual Assur*. 2008;13:335–337.
58. Fagerholm PP, Philipson BT, Lindström B. Normal human lens—the distribution of protein. *Exp Eye Res*. 1981;33:615–620.
59. Christiansen P, Toft PB, Gideon P, Danielsen ER, Ring P, Henriksen O. MR-visible water content in human brain: a proton MRS study. *Magn Reson Imaging*. 1994;12:1237–1244.
60. Kreis R. Quantitative localized 1H MR spectroscopy for clinical use. *Prog Nucl Magn Reson Spectrosc*. 1997;31:155–195.
61. Ernst T, Kreis R, Ross B. Absolute quantitation of water and metabolites in the human brain. I. Compartments and water. *J Magn Reson B*. 1993;102:1–8.
62. Rácz P, Tompa K, Pócsik I. The state of water in normal and senile cataractous lenses studied by nuclear magnetic resonance. *Exp Eye Res*. 1979;28:129–135.
63. Rácz P, Tompa K, Pócsik I. The state of water in normal human, bird and fish eye lenses. *Exp Eye Res*. 1979;29:601–608.
64. Rácz P, Tompa K, Pócsik I, Bánki P. Water fractions in normal and senile cataractous eye lenses studied by NMR. *Exp Eye Res*. 1983;36:663–669.
65. Pope JM, Chandra S, Balfe JD. Changes in the state of water in senile cataractous lenses as studied by nuclear magnetic resonance. *Exp Eye Res*. 1982;34:57–63.
66. Patz S, Bert RJ, Frederick E, Freddo TF. T(1) and T(2) measurements of the fine structures of the in vivo and enucleated human eye. *J Magn Reson Imaging*. 2007;26:510–518.
67. Richdale K, Wassenaar P, Teal Bluestein K, et al. 7 Tesla MR imaging of the human eye in vivo. *J Magn Reson Imaging*. 2009;30:924–932.
68. Bushberg JT, Seibert JA, Leidholdt EM, Jr, Boone JM. *The Essential Physics of Medical Imaging*. 3rd ed. Wolters Kluwer Health/Lippincott Williams & Wilkins; 2012.
69. Hains PG, Truscott RJW. Post-translational modifications in the nuclear region of young, aged, and cataract human lenses. *J Proteome Res*. 2007;6:3935–3943.
70. Wilmarth PA, Tanner S, Dasari S, et al. Age-related changes in human crystallins determined from comparative analysis of post-translational modifications in young and aged lens: does deamidation contribute to crystallin insolubility? *J Proteome Res*. 2006;5:2554–2566.
71. Bloemendal H, de Jong W, Jaenicke R, Lubsen NH, Slingsby C, Tardieu A. Ageing and vision: structure, stability and function of lens crystallins. *Prog Biophys Mol Biol*. 2004;86:407–485.
72. Harrington V, McCall S, Huynh S, Srivastava K, Srivastava OP. Crystallins in water soluble-high molecular weight protein fractions and water insoluble protein fractions in aging and cataractous human lenses. *Mol Vis*. 2004;10:476–489.
73. Gao J, Sun X, Moore LC, Brink PR, White TW, Mathias RT. The effect of size and species on lens intracellular hydrostatic pressure. *Invest Ophthalmol Vis Sci*. 2013;54:183–192.
74. Gao J, Sun X, Moore LC, White TW, Brink PR, Mathias RT. Lens intracellular hydrostatic pressure is generated by the circulation of sodium and modulated by gap junction coupling. *J Gen Physiol*. 2011;137(6):507–520.
75. Donaldson PJ, Kistler J, Mathias RT. Molecular solutions to mammalian lens transparency. *News Physiol Sci*. 2001;16:118–123.
76. Mathias RT, Rae JL, Baldo GJ. Physiological properties of the normal lens. *Physiol Rev*. 1997;77:21.
77. Mathias RT, Kistler J, Donaldson P. The lens circulation. *J Membr Biol*. 2007;216:1–16.
78. Gao J, Sun X, White TW, Delamere NA, Mathias RT. Feedback regulation of intracellular hydrostatic pressure in surface cells of the lens. *Biophys J*. 2015;109:1830–1839.
79. Bettelheim FA. Syneretic response to pressure in ocular lens. *J Theor Biol*. 1999;197:277–280.
80. Bettelheim FA, Lizak MJ, Zigler JSJ. NMR relaxation studies of syneretic response to pressure change in bovine lenses. *Curr Eye Res*. 2001;22:438–445.

Investigative Ophthalmology & Visual Science

81. Bettelheim FA, Lizak MJ, Zigler JS, Jr. Syneretic response of aging normal human lens to pressure. *Invest Ophthalmol Vis Sci*. 2003;44:258–263.
82. Schachar R. Letter to the Editor: Accommodation, presbyopia, and the lenticular syneretic response. *Curr Eye Res*. 2005;30:927.
83. Augusteyn RC. On the growth and internal structure of the human lens. *Exp Eye Res*. 2010;90:643–654.
84. Chen Y, Gao J, Li L, et al. The ciliary muscle and zonules of Zinn modulate lens intracellular hydrostatic pressure through transient receptor potential vanilloid channels. *Invest Ophthalmol Vis Sci*. 2019;60:4416–4424.
85. Dubbelman M, Van der Heijde GL, Weeber HA, Vrensen GFJM. Changes in the internal structure of the human crystalline lens with age and accommodation. *Vis Res*. 2003;43:2363–2375.
86. Hermans E, Dubbelman M, van der Heijde R, Heethaar R. The shape of the human lens nucleus with accommodation. *J Vis*. 2007;7:16 1–10.
87. Koretz JF, Cook CA, Kaufman PL. Accommodation and presbyopia in the human eye. Changes in the anterior segment and crystalline lens with focus. *Invest Ophthalmol Vis Sci*. 1997;38:569–578.

Investigative Ophthalmology & Visual Science